

IMITATIONAL SIMULATION OF CUMULUS CLOUDS FOR STUDYING SOLAR RADIATIVE TRANSFER IN THE ATMOSPHERE BY THE MONTE CARLO METHOD

B.A. Kargin and S.M. Prigarin

*Computer Center,
Siberian Branch of the Russian Academy of Sciences, Novosibirsk
Received January 4, 1994*

Algorithms for numerical simulation of stochastic cumulus cloud fields are developed for solving some problems of atmospheric optics. A new method is proposed to simulate broken clouds for spectral models of uniform Gaussian fields.

Studies in the fields of atmospheric general circulation, climate, and meteorology as well as a large number of applied problems of atmospheric optics call for the development of imitational models of stochastic cloud fields. Broken clouds are the most difficult object to simulate. In this regard methods of numerical simulation of random processes and fields seem to be most promising for simulation of the stochastic geometry and inner structure of broken clouds.

In the present paper, we develop and investigate so-called Gaussian models of broken clouds and use them to study solar radiative transfer in the atmosphere by the Monte Carlo method. In addition to advantages in common with some other existing geometric models of broken clouds (see, e.g., Refs. 1 and 2 as well as reviews in Refs. 3 and 4), Gaussian models have their own advantages, above all, due to efficient numerical algorithms, fast adjustment of model to the basic cloud parameters, and a great variety of reproducible geometric shapes.

In this paper, the Gaussian models are compared with cumulus cloud model based on the approximation of clouds by truncated convex paraboloids. Optical characteristics calculated for different cloud models are presented. Results of computational experiment are compared with asymptotic results obtained in Ref. 5 for the probability of radiation transmission through a stochastic medium.

1. FORMULATION OF THE PROBLEM

To describe the process of radiative transfer, the integral equation of the second kind with the generalized kernel⁶

$$\varphi(\kappa) = \int_X K(\kappa', \kappa) \varphi(\kappa') d\kappa' + f(\kappa), \quad (1)$$

$$K(\kappa', \kappa) = \frac{\beta(r') g(\mu, r') \exp(-\tau(r', r)) \sigma(r)}{2\pi \|r - r'\|^2 \sigma(r')} \delta\left(\omega - \frac{r - r'}{\|r - r'\|}\right),$$

is used, where $\varphi(\kappa)$ is the collision density, $\varphi(\kappa) = \sigma(r)\Phi(\kappa)$; $\Phi(\kappa) = \Phi(r, \omega)$ is the radiant flux density (intensity) at the point r in the direction ω ; $\kappa = (r, \omega)$ and $\kappa' = (r', \omega')$ are the points in the phase space; $X = \{r \in R \subset R^3, \omega = (a, b, c), a^2 + b^2 + c^2 = 1\}$; $\mu = \langle \omega', r - r' \rangle / \|r - r'\|$ is the cosine of scattering angle; $g(\mu, r)$ is the scattering phase function, $\int_{-1}^1 g(\mu, r) d\mu = 1$; $\tau(r', r) = \int_0^l \sigma(r(t)) dt$ is the

optical depth of the segment $[r', r]$, $r(t) = r' + t(r - r')/l$, $l = \|r - r'\|$; $\sigma(r) = \alpha(r) + \beta(r)$ is the extinction coefficient; $\alpha(r)$ is the absorption coefficient; $\beta(r)$ is the scattering coefficient; $f(\kappa)$ is the source density function.

To calculate functionals of the solution of the transfer equation, the characteristics of a medium $\alpha(r)$, $\beta(r)$, and $g(\mu, r)$ as well as those of a source $f(\kappa)$ must be known. General methods and algorithms for statistical simulation of radiative transfer are well-known from a large body of literature (see, e.g., Refs. 6 and 7).

The process of optical radiative transfer in a cloud layer is described by a system of single-parameter uncoupled equations (1), with the parameter $\lambda \in [\Lambda_1, \Lambda_2]$ representing the wavelength.

The region R is taken to be the plane layer

$$R = \{r = (x, y, z); H_1 \leq z \leq H_2\},$$

and the source is considered as the plane-parallel flux in the direction ω_0

$$f_\lambda(\kappa) = S_0(\lambda) \delta(z - H_2) \delta(\omega - \omega_0),$$

$$\omega_0 = (a_0, b_0, c_0), \quad c_0 = -\cos \theta_0 < 0,$$

where $S_0(\lambda)$ is the spectral distribution of incident radiation and θ_0 is the angle between the vertical axis OZ and the incident rays.

As is well known, selective absorption by atmospheric gases is of importance for optical radiative transfer in some sections of the spectrum along with Rayleigh and aerosol extinction, it cannot be described by the linear radiative transfer theory and requires the use of the transmission function $P_{\Delta\lambda}(L)$ (see, e.g., Refs. 6 and 7). The transmission function has the meaning of the probability of photon "survival" on the path L . In what follows the transmission function $P_{\Delta\lambda}(L)$ is completely determined by the effective (reduced) mass of absorber on the path L . The effective absorber mass is defined as

$$m(L) = \int_L \rho(r) [p(r)/p_0]^\gamma dl,$$

where $\rho(r)$ is the absorber density at the point r ; $p(r)$ and p_0 are the air pressures at the point r and at the surface, respectively; $0 \leq \gamma \leq 1$.

A notable feature of the problem is the stochastic and not deterministic structure of the medium. That is, the

functions $\alpha(r)$, $\beta(r)$, and $g(\mu, r)$ are realization of random fields, and their simulation is the main purpose in the case considered. Stochasticity of the medium makes the Monte Carlo method the only one suitable to solve the problem.

2. GEOMETRIC MODELS OF CUMULUS CLOUDS AND SIMULATION ALGORITHMS

2.1. Gaussian models

It was hypothesized in Ref. 9 that cumulus clouds can be described using a stationary Gaussian process. This hypothesis provided a basis for construction of the theoretical–experimental model of statistical structure of cumulus clouds (see Refs. 10 and 11, Chap. 3). The numerical model of cloud structure based on this hypothesis was first constructed in Ref. 12 for statistical simulation of optical radiative transfer. The Gaussian models were further developed and studied in Ref. 13.

2.1.1. Description of models. Let us assume that the cloudiness is bounded at its bottom by the plane $z = H_0$ (the cloud lower boundary determined by the condensation level varies only slightly in space), while the cloud upper boundary $z = \omega(x, y)$ is defined by the formula (model G_1)

$$\omega(x, y) = H_0 + \max(\sigma [v(x, y) - d], 0), \tag{2}$$

where $d \in (-\infty, +\infty)$, $\sigma > 0$, $v(x, y)$ is the uniform Gaussian random field with zero mean, unit variance, and correlation function $K(x, y)$. The absolute cloud–cover index n_0 is defined as

$$n_0 = 1 - \Phi(d), \tag{3}$$

where Φ is the function of the standard normal distribution.

A feature of model (2) is that for $d \leq 0$ ($n_0 \geq 0.5$) cloud configuration matches the structure of stratus clouds with gaps. For this reason the model G_2

$$\omega(x, y) = H_0 + \max(\sigma [|v(x, y)| - d], 0), \quad d \geq 0. \tag{4}$$

was proposed for modeling cumulus clouds in addition to model (2). In this case

$$n_0 = 2(1 - \Phi(d)). \tag{5}$$

In addition to the cloud–cover index n_0 , we introduce the mean cloud amount m_0 per unit area and the mean cloud thickness h_0 . According to formula (45.51) from Ref. 14 we have

$$m_0 = (2\pi)^{-3/2} d (k_{20} k_{02} - k_{11}^2)^{1/2} \exp(-d^2 / 2), \tag{6}$$

where $d > 0$ for model (2), and

$$m_0 = 2(2\pi)^{-3/2} d (k_{20} k_{02} - k_{11}^2)^{1/2} \exp(-d^2 / 2) \tag{7}$$

for model (4). Here

$$k_{ij} = - \left. \frac{\partial K(x, y)}{\partial x^i \partial y^j} \right|_{x=y=0}.$$

The Gaussian cloud models (2) and (4) are uniquely determined by the values of d and σ and the correlation function $K(x, y)$. Fitting these parameters appropriately, one easily adjusts the model to a required cloud–cover index and mean vertical and horizontal cloud extent. This allows the models (2) and (4) to be used for simulation of different structure of cumulus and wave clouds (Fig. 1). Moreover, uniform random fields can be used to construct models for stratified cloudiness with stochastic upper and lower boundaries.

2.1.2. Numerical simulation algorithms. Numerical construction of the stochastic structure of broken clouds for models (2) and (4) reduces to modeling of a uniform Gaussian field $v(x, y)$ with a given correlation function. We modeled using the method of spectrum randomization¹⁵ or, more precisely, its modification for isotropic fields (see Refs. 16 and 17), for it is reasonable to consider first the isotropic cloudiness case, which is easily extended to nonisotropic structures by scaling along one of the coordinate axes.

For isotropic case $k_{20} = k_{02}$ and $k_{11} = 0$, and formulas (6) and (7) become respectively

$$m_0 = (2\pi)^{-3/2} d k_{02} \exp(-d^2 / 2), \quad d \geq 0, \tag{8}$$

$$m_0 = 2(2\pi)^{-3/2} d k_{02} \exp(-d^2 / 2). \tag{9}$$

The spectral measure of isotropic field in the plane possesses the circular symmetry, and the correlation function can be represented as

$$K(x, y) = B(r) = \int_0^\infty J_0(\rho r) \mu(d\rho), \tag{10}$$

where $r^2 = x^2 + y^2$; J_0 is the Bessel function of the first kind; $\mu(d\rho)$ is the radial spectral measure on $[0, \infty)$. (The table of spectral measures and corresponding correlation functions for isotropic fields are given in Ref. 18.) In this case

$$k_{02} = 2^{-1} \int_0^\infty \rho^2 \mu(d\rho).$$

Below we discuss the algorithms for numerical simulation of uniform Gaussian isotropic fields in a plane proposed in Refs. 16 and 17.

Suppose $0 = R_0 < R_1 < \dots < R_{N-1} < R_N = \infty$. For the approximate model of the Gaussian field $v(x, y)$ with correlation function (10) we use

$$v^*(x, y) = \sum_{n=1}^N c_n M_n^{-1/2} \sum_{m=1}^{M_n} (-2 \ln \alpha_{nm})^{1/2} \times \\ \times \cos [x \rho_n \cos \omega_{nm} + y \rho_n \sin \omega_{nm}] + 2\pi \beta_{nm}, \tag{11}$$

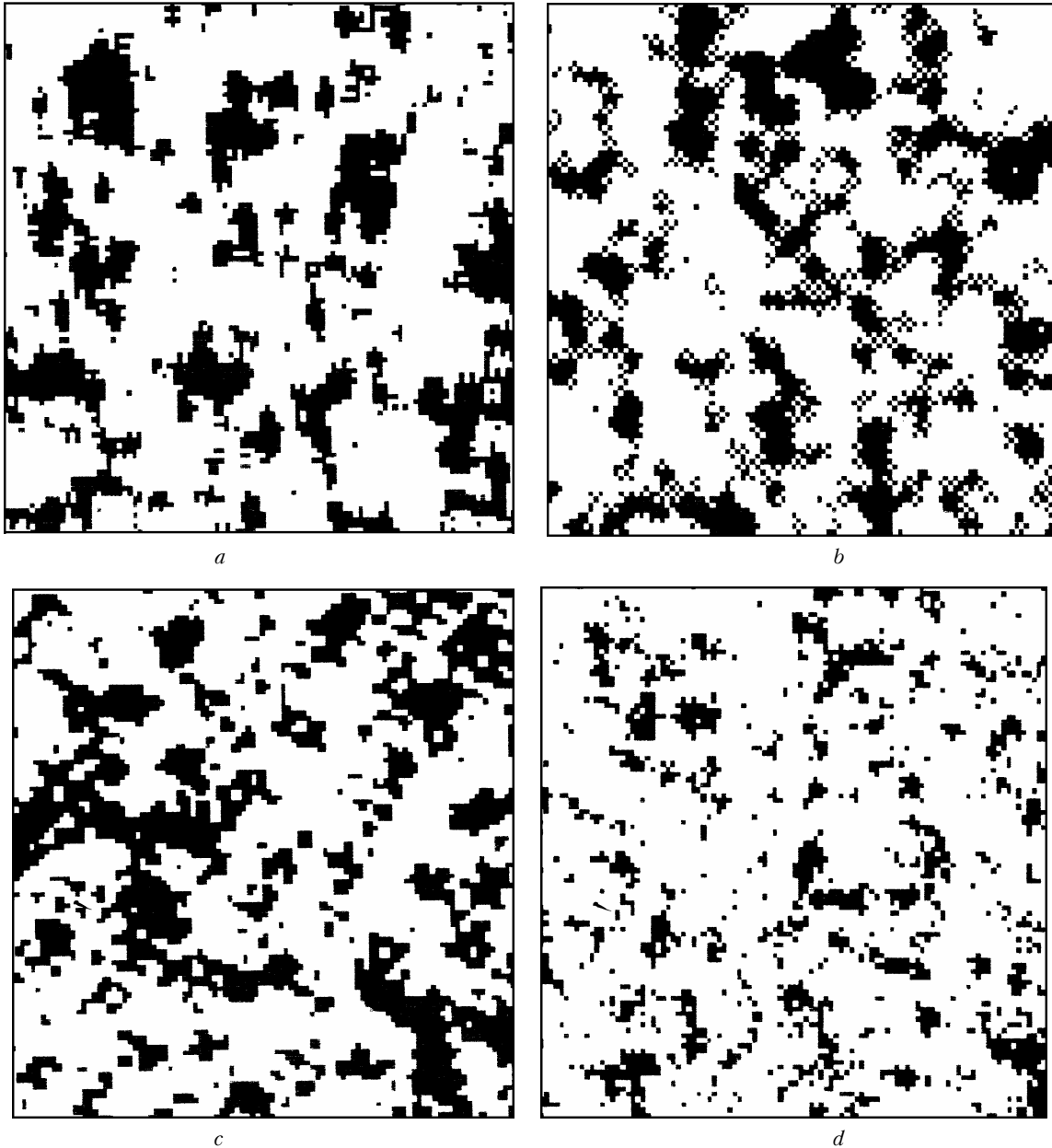


FIG. 1. Illustrative realization of Gaussian cloud models (cloud base configuration).

Where $c_n^2 = \int_{R_{n-1}}^{R_n} \mu(d\rho)$; $\omega_{nm} = \pi(m - \gamma_{nm})/M_n$;

ρ_n are the random variables distributed over $[R_{n-1}, R_n)$ with measure $\mu(d\rho)$; α_{nm} , β_{nm} , and γ_{nm} are independent random variables distributed uniformly over $[0, 1]$.

Modeling algorithm calculates the arrays

$$A(n, m) = c_n (-2(\ln \alpha_{nm})/M_n)^{1/2}, \quad D(n, m) = 2\pi\beta_{nm},$$

$$B(n, m) = \rho_n \cos \omega_{nm}, \quad C(n, m) = \rho_n \sin \omega_{nm},$$

while the magnitude of the field at a desired point (x, y) is obtained from the formula

$$v^*(x, y) = \sum_{n=1}^N \sum_{m=1}^{M_n} A(n, m) \cos [B(n, m)x + C(n, m)y + D(n, m)].$$

In model (11) the spectral space is partitioned into rings, and each ring is partitioned into equal segments. The correlation function for model (11) is given by Eq. (10), and when $\sum_{n=1}^N M_n \rightarrow \infty$ so that $\max_{n \leq N} (c_n^2/M_n) \rightarrow \infty$, the field $\omega^*(x, y)$ is asymptotically Gaussian.

The other variants of the spectral model are possible. In particular, by the following substitutions in Eq. (11) (separately or in combinations): 1) $\rho_n = \rho_{nm}$, 2) $\gamma_{nm} = \gamma_n$,

and 3) $\gamma_{nm} = \gamma$, where ρ_{nm} , γ_n , and γ are independent random variables with pertinent distributions. The first replacement may be particularly useful when $n = N$.

Model (11) is algorithmically simpler but less flexible, where $c_n = N^{-1/2}$, and ρ_n are independent and distributed over the entire semiaxis $[0, \infty)$ with measure $\mu(d\rho)$. Computer realization of this algorithm is presented in Ref. 17.

Choice of simulation algorithm and its parameter values depends on our desire to translate more or less fully relevant sections of the spectrum and affects the character of $v^*(x, y)$ realization.

For computations we chose the simplest correlation function for isotropic field

$$K(x, y) = J_0(\rho(x^2 + y^2)^{1/2}), \tag{12}$$

and modeled approximately the Gaussian field using the formula

$$v^*(x, y) = M^{-1/2} \sum_{i=1}^M (-2 \ln \alpha_i)^{1/2} \times \cos [x \rho \cos \omega_i + y \rho \sin \omega_i + 2 \pi \beta_i], \tag{13}$$

where $\omega_i = \pi(i + \alpha')/M$ (α' , α_i , and β_i are the random variables uniformly distributed over $[0, 1]$). The computer program calculates the arrays

$$A(i) = (-2(\ln \alpha_i)/M)^{1/2}, \quad B(i) = \rho \cos \omega_i, \\ C(i) = \rho \sin \omega_i, \quad D(i) = 2 \pi \beta_i,$$

and the field magnitude at a desired point (x, y) is obtained by the formula

$$v^*(x, y) = \sum_{i=1}^M A(i) \cos [B(i)x + C(i)y + D(i)].$$

Formulas (8) and (9) for correlation function (12) yield, respectively

$$m_0 = 2^{-1} (2\pi)^{-3/2} d \rho^2 \exp(-d^2/2), \quad d > 0 \tag{14}$$

$$m_0 = (2\pi)^{-3/2} d \rho^2 \exp(-d^2/2). \tag{15}$$

2.1.3. Adjustment of models. The mean cloud thickness h_0 and the parameters of model (4) for correlation function (12) are related as

$$h_0 = \sigma \int_d^{+\infty} (h-d) p(h) dh / \int_d^{+\infty} p(h) dh, \tag{16}$$

where $h > 0$ and $p(h) = 2(2\pi/3)^{-1/2}(h^2 - 1 + e^{-h^2}) \exp(-h^2/2)$ is the density function of magnitudes of local maxima of Gaussian field with correlation function (12) (see Ref. 19).

Comment. Expediency of the use of the density function of isotropic Gaussian field local maxima for mean cloud thickness computation in the case of correlation function defined by Eq. (12) was justified by numerical experiment. The use of Eq. (16) for arbitrary correlation function may be unjustified (we note in this regard that the authors of Ref. 20 inaccurately reported the material borrowed from Ref. 13).

Now the algorithm for specifying the parameters of model (4) and (12) starting from the given cloud characteristics n_0 , h_0 , and m_0 is as follows. First, we find d from Eq. (5), then calculate σ using Eq. (16). Finally, knowing m_0 , we determine ρ from Eq. (15). The model (2) and (12) is adjusted in the same way.

We note that familiar properties of random fields can be used to study various characteristics of models (2) and (4). For instance, the formula for calculating the mean length of the cloud base contour can be derived from the results of Ref. 14, while the formula for the mean cloud amount per unit area – from Ref. 21 (see p. 182).

2.1.4. On the choice of correlation function. As has already been noted, test calculations were made for cloud models based on the uniform Gaussian isotropic fields with simplest correlation function (12). However, some numerical experiments call for more complex models, so adjusted that to fit the real cloud field configurations of different types. We now describe one possible method of choosing the correlation function $K(x, y)$ in models (2) and (4) using observations.

Let us suppose that we have cloud field images in a plane that can be interpreted as uniform random indicator fields $\varepsilon(x, y)$, with $\varepsilon(x, y) = 1$ indicating the presence of a cloud at the point (x, y) and $\varepsilon(x, y) = 0$ indicating that the point (x, y) is located in the gap between clouds. For better correspondence between model cloud field configurations and configurations of really observed fields $\varepsilon(x, y)$, the correlation function $K(x, y)$ for model (2) should be taken as follows:

$$K(x, y) = R^{-1}(B(x, y)), \tag{17}$$

where $B(x, y)$ is the covariance function calculated using $\varepsilon(x, y)$, $B(x, y) \approx M\varepsilon(0, 0)\varepsilon(x, y)$, and the function R is given by the formula

$$R(\rho) = \iint_{-\$}^{+\infty} u(\xi) u(\eta) \varphi_\rho(\xi, \eta) d\xi d\eta, \tag{18}$$

$$\varphi_\rho(\xi, \eta) = \left[2\pi \sqrt{1 - \rho^2} \exp\left(\frac{\xi^2 + \eta^2 - 2\rho\xi\eta}{2(1 - \rho^2)}\right) \right]^{-1},$$

$$u(x) = \begin{cases} 1, & \text{for } x \geq d, \\ 0, & \text{for } x < d. \end{cases}$$

(Recall that Φ denotes the function of standard normal distribution.) This procedure for calculating the correlation function $K(x, y)$ corresponds to the well-known method of inverse distribution function used in statistical simulation (see Refs. 22 and 23). Note that at $d = 0$ and $n_0 = 0.5$ Eq. (18) yields $R(\rho) = 1/4 + (2\pi)^{-1} \arcsin \rho$.

For model (4) we also use Eqs. (17) and (18) with

$$u(x) = \begin{cases} 1, & \text{for } |x| \geq d, \\ 0, & \text{for } |x| < d. \end{cases}$$

2.2. Paraboloid cloud model (model P)

An alternative geometric description of cumulus cloudiness is based on the fact that real cumulus clouds are typically shaped as truncated convex paraboloids.^{24,25}

Cloud base centers (A_i, B_i) are simulated uniformly over $[OX] \times [OX]$. The distribution of cumulus cloud diameters is approximated by lognormal or beta

distribution.²⁶ Cloud base radii R_i are simulated with the density function¹¹

$$p(R) = \begin{cases} 9.66329 R(1-R/1.875)^{4.35}, & R \leq 1.875 \text{ km}, \\ 0, & R > 1.875 \text{ km}. \end{cases} \quad (19)$$

Modeling formula for beta distribution can be found in Ref. 22. In the case considered it is of the form

$$R = 1.875 \left\{ 1 - (\alpha_1 \alpha_2)^{[\alpha_3/5.35 + (1 - \alpha_3)/6.35]} \right\},$$

where α_1 and α_2 are uniformly distributed on $[0, 1]$. Cloud thicknesses H_i are chosen as²⁴

$$H_i = 1.91 R_i (R_i/1.875)^{-0.031}. \quad (20)$$

The point (x, y, z) is within the cloud when for some $i \in \{1, 2, \dots, m\}$ (with m being the number of clouds contained in the area X^2) we have

$$H_0 < z < H_i - C_i[(x - A_i)^2 + (y - B_i)^2] + H_0, \quad C_i = H_i/R_i^2,$$

where H_0 is the height of the lower boundary of cloudiness.

Simulation admits paraboloid overlapping, and base centers are simulated with the help of the Poisson point process on a plane with intensity λ (i.e., the probability that just m points find themselves within the area S is $\exp(-\lambda S)(\lambda S)^m/m!$). In case of constant base radii ($R_i = R_0$), the cloud-cover index is given by the expression²

$$n_0 = 1 - \exp(-\lambda \pi R_0^2).$$

When the radii are distributed at random with the probability density $p(R)$, for the cloud-cover index we have²⁷

$$n_0 = 1 - \exp(-\lambda \pi \langle R^2 \rangle), \quad \langle R^2 \rangle = \int_0^{R_{\max}} r^2 p(r) \, d r.$$

(For Eq. (19) we have $\langle R^2 \rangle = 0.3437 \text{ km}^2$.)

Thus the model P is determined by the cloud-cover index n_0 , relations (19) and (20), and the parameter X . The main shortcoming of paraboloid models in comparison with Gaussian ones is that they require greater computer time for larger n_0 and X .

2.3. Additional comments on models of broken cloudiness

It seems promising to simulate broken cloudiness with the help of models using nonlinear transformations of Gaussian random fields in space. Conceivably this approach will be more adequate for simulating cloud field geometry; however, these models are cumbersome and call for additional profound mathematical investigation. An interesting approach to simulation of cumulus clouds suggested in Ref. 20 should be mentioned here, which is based on the combination of paraboloid and Gaussian models. However, the problem with this approach is the model adjustment (e.g., to a cloud thickness and, particularly, to an absolute cloud-cover index). Finally, the problem of reproducing cloud fractal dimensionality touched on in Ref. 20, can easily be solved for Gaussian models.

3. EVALUATION OF RADIATIVE CHARACTERISTICS OF CUMULUS CLOUDS BY THE MONTE CARLO METHOD

3.1. Radiative characteristics of cumulus clouds computed over the visible wavelength range $0.4 \leq \lambda \leq 0.72 \text{ }\mu\text{m}$

Scattering and absorption in the cloudless atmosphere were neglected in computations. Clouds were assumed to be a scattering medium with $\sigma = 30 \text{ km}^{-1}$. The scattering phase function was borrowed from Ref. 11, Chap. 4. Photon trajectories were simulated by the method of maximum cross section. Cumulus clouds were modeled using model (4) and (12) with the parameters: the angle between the vertical axis and incident beam ψ_0 ; $\theta_0 = 180^\circ - \psi_0$; the absolute cloud-cover index n_0 ; the mean cloud thickness h_0 ; the characteristic diameter of cloud base d_0

$$\pi(d_0/2)^2 = n_0/m_0.$$

The following radiative characteristics were calculated: the albedo of cloud system A , the fraction of the scattered transmitted radiation T , and the direct solar radiation transmitted through the clouds S , where $A + T + S = 1$. The uniform Gaussian field with correlation function (12) was simulated approximately using formula (13) for $M = 10$ (further increase of M scarcely affects the results).

The results of calculations are presented in Table I and shown in Figs. 2 and 3. Figure 2 illustrates the dependence of A , T , and S on θ_0 for $n_0 = 0.5$, $h_0 = 0.5 \text{ km}$, and $d_0 = 0.7 \text{ km}$.

TABLE I. Radiative characteristics for the model G_2 with different parameters θ_0 , h_0 , and d_0 .

θ_0 , deg	h_0 , km	d_0 , km	n_0	A , %	T , %	S , %	T/A
45	1	1	0.3	18	24	58	1.34
			0.5	27	38	35	1.40
			0.7	37	47	16	1.27
			0.9	47	51	2	1.09
60	0.5	0.25	0.1	8	22	70	2.75
			0.3	19	48	33	2.53
			0.5	27	62	11	2.30
			0.7	33	65	2	1.97
			0.9	42	58	0	1.38

Note that for $n_0 \leq 0.7$ the ratio T/A remains practically unchanged (see upper rows of Table I). This fact shows that radiation fields of individual clouds are practically noninteracting. As the cloud-cover index increases, the ratio T/A decreases. The effect is stronger for higher ratio h_0/d_0 and at larger θ_0 (see lower rows of Table I).

Figure 3 depicts the dependence of A , T , and S on cloud horizontal size at $\theta_0 = 45^\circ$ for $n_0 = 0.5$ and $h_0 = 0.5 \text{ km}$. As d_0 increases, the fraction of direct radiation increases, the scattered transmitted radiation decreases, and the albedo slightly decreases.

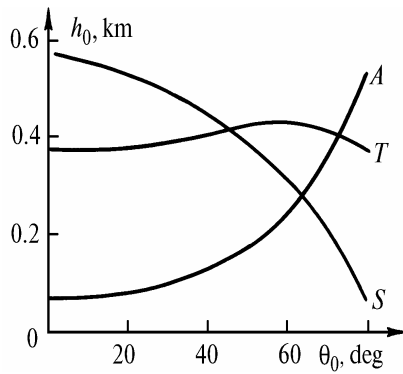


FIG. 2. The dependence of albedo (A), fraction of the scattered transmitted radiation (T), and direct radiation transmitted through the clouds (S) on the angle of incidence of solar rays (θ₀ is the angle between the outward normal to the atmospheric surface and the direction toward the source, n₀ = 0.5, h₀ = 0.5 km, and d₀ = 0.7 km)

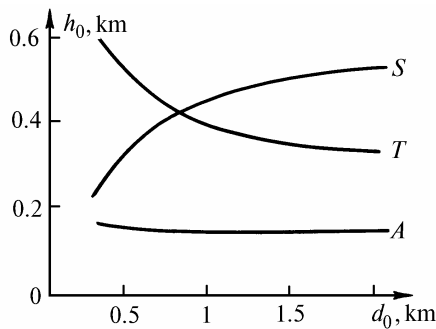


FIG. 3. The dependence of albedo (A), fraction of the scattered transmitted radiation (T), and direct radiation transmitted through the clouds (S) on characteristic cloud base diameter (θ₀ = 45°, n₀ = 0.5, and h₀ = 0.5 km).

Table II summarizes the results computed for models G₁, G₂, and P for n₀ = 0.2, h₀ = 1 km, and d₀ = 1 km.

TABLE II. Radiative characteristics for three cloud models.

θ, deg	Characteristics, %								
	A			T			S		
	Model								
	G ₁	G ₂	P	G ₁	G ₂	P	G ₁	G ₂	P
0	5	6	8	14	12	12	81	82	80
20	6	6	8	14	14	11	80	80	81
40	10	12	12	18	17	12	72	71	76
60	17	18	15	23	18	15	60	64	70
80	47	45	48	27	22	20	26	33	32

3.2. Comparison of simulation results with asymptotic results of Mikhailov

For model G₁ and vertical incident radiation it was proposed in Ref. 28 to use the asymptotic results from Ref. 5 to estimate the solar intensity transmitted through the clouds. Using model G₁ described by Eqs. (2) and (12) and asymptotic function from Ref. 5, we calculated the

probabilities of photon transmission through the cloudiness for the model problem with the scattering phase function in the transport approximation, mean cosine of the scattering angle of 0.9, and single scattering albedo of 0.7 (σ=30 km⁻¹). For n₀ ≥ 0.5, a good agreement between the results was obtained.

TABLE III. Probabilities of photon transmission through the clouds (model G₁).

n ₀	Mτ	(Dτ) ^{1/2}	Transmission probability, %	
			1	2
3	4.33	9.20	88	75
4	5.38	9.37	71	66
5	6.50	9.52	57	58
6	7.71	9.58	46	49
7	9.07	9.53	37	39
8	10.67	9.32	27	30
9	12.77	8.79	17	17

Note: Here n₀ is the cloud-cover index, Mτ is the mean optical thickness of the layer, Dτ is the variance of optical thickness, columns 1 and 2 list the asymptotic results borrowed from Ref. 5 and the results of simulation using formulas (2) and (12).

3.3. Simulation of radiative transfer in the near-IR spectral range

Cloud absorptance in the near-IR range of solar spectrum is primarily determined by water vapor and water content. The model G₁ was tested for a cloud layer of 1 km thickness (with parameters n₀ = 0.4, h₀ = 0.5 km, d₀ = 0.7 km, water content in clouds ρ_w = 0.3 g/m³, and absolute humidity inside clouds 7.5 g/m³ and outside clouds 5 g/m³) in the wavelength range λ ∈ (1.66 μm and 2.08 μm). The scattering phase function was borrowed from Ref. 11 (see p. 47). The transmission function was calculated using the formula

$$P(m_v, m_w) = P(m_v) \exp(-\alpha_w m_w),$$

where α_w = 61.05 cm²/g, while the values of P(m_v) can be found in Ref. 11 (see p. 71). Table IV presents the dependence of the cloud layer albedo and absorption on the angle θ₀ (with a scattering coefficient of 30 km⁻¹). Photon trajectories were simulated by the method of maximum cross section, while the effective absorber mass was calculated by dividing each trajectory into segments 50 m long.

TABLE IV. Cloud layer albedo A and absorptance Ab within the water vapor absorption band Ω.

θ ₀ , deg	α _w , cm ² /g			
	61.05*		0**	
	A, %	Ab, %	A, %	Ab, %
0	3	41	6	34
20	4	43	7	35
40	6	49	12	37
60	11	55	19	40
80	22	60	36	45

* with regard for absorption by water vapor
 ** without regard

ACKNOWLEDGMENTS

This work was sponsored by the Russian Fund of Fundamental Researches (Grant No. 93-012-500).

REFERENCES

1. O.A. Avaste et al., in: *Monte Carlo Methods in Computational Mathematics and Mathematical Physics* (Novosibirsk, 1974), pp. 332-239.
2. G.A. Titov, *Opt. Atm.* **1**, No. 4, 3-18 (1988).
3. G.A. Titov, "Statistical description of optical radiative transfer in clouds," Doctoral Thesis in Physical and Mathematical Sciences, Institute of Atmospheric Optics, Tomsk (1989), 361 pp.
4. T.B. Zhuravleva, "Statistical characteristics of solar radiation in broken clouds," Candidate's Dissertation in Physical and Mathematical Sciences, Institute of Atmospheric Optics, Tomsk (1993), 158 pp.
5. G.A. Mikhailov, *Izv. Akad. Nauk SSSR, ser. Fiz. Atmos. Okeana* **18**, No. 12, 1289-1295 (1982).
6. G.I. Marchuk, et al., *Monte Carlo Method in Atmospheric Optics* (Nauka, Novosibirsk, 1976), 283 pp.
7. B.A. Kargin, *Statistical Simulation of Solar Radiation Field in the Atmosphere*, Computer Center of the Siberian Branch of the Academy of Sciences of the USSR, Novosibirsk (1984), 206 pp.
8. V.E. Zuev and G.M. Krekov, *Optical Models of the Atmosphere* (Gidrometeoizdat, Leningrad, 1986), 256 pp.
9. Yu.-A.R. Mullamaa, in: *Radiation and Clouds*, IFA Akad. Nauk ESSR, Tartu (1969), pp. 10-20.
10. Yu.-A.R. Mullamaa, M.A. Sulev, V.K. Pyldmaa, et al., *Stochastic Structure of Cloud and Radiation Fields*, IFA Akad. Nauk ESSR, Tartu (1972), 281 pp.
11. E.M. Feigel'son, ed., *Radiation in the Cloudy Atmosphere* (Gidrometeoizdat, Leningrad, 1981), 280 pp.
12. B.A. Kargin and S.M. Prigarin, "Simulation of stochastic fields of cumulus clouds and the study of their radiative properties by the Monte Carlo method," Preprint No. 817, Computer Center of the Siberian Branch of the Academy of Sciences of the USSR, Novosibirsk (1988), 18 pp.
13. S.M. Prigarin, "Simulation of random fields and solution of some stochastic problems of atmospheric optics by the Monte Carlo method," Candidate's Dissertation in Physical and Mathematical Sciences, Computer Center of the Siberian Branch of the Academy of Sciences of the USSR, Novosibirsk (1990), 125 pp.
14. A.A. Sveshnikov, *Applied Methods in the Theory of Random Functions* (Nauka, Moscow, 1968), 320 pp.
15. G.A. Mikhailov, *Dokl. Akad. Nauk SSSR* **238**, No. 4, 793-795 (1978).
16. S.M. Prigarin, in: *Abstracts of Reports at the All-Union Scientific-Technical Conference on Identification and Measurements of the Characteristics and Simulation of Random Processes*, Novosibirsk (1991), pp. 38-39.
17. S.M. Prigarin, "Spectral methods for uniform vector fields," Preprint No. 945, Computer Center of the Siberian Branch of the Academy of Sciences of the USSR, Novosibirsk (1992), 36 pp.
18. S.M. Prigarin, in: *Theory of Statistical Simulation and its Applications* (Novosibirsk, 1989), pp. 64-78.
19. V.I. Tikhonov, *Nonlinear Transformations of Random Processes* (Radio i Svyaz', Moscow, 1980), 250 pp.
20. E.A. Babich and G.A. Titov, *Atmos. Oceanic Opt.* **5**, No. 7, 478-484 (1992).
21. A.P. Khusu, Yu.R. Vitenberg, and V.A. Pal'mov, *Surface Roughness. Theoretical-Probabilistic Approach* (Nauka, Moscow, 1975), 300 pp.
22. S.M. Ermakov and G.A. Mikhailov, *Statistical Simulation* (Nauka, Moscow, 1982), 296 pp.
23. S.M. Prigarin, in: *Statistical Simulation Techniques* (Novosibirsk, 1986), pp. 3-15.
24. V.G. Plank, *J. Meteorol.* **8**, No. 1, 46-67 (1969).
25. E.M. Feigel'son and L.D. Krasnokutskaya, *Solar Radiation Fluxes and Clouds* (Gidrometeoizdat, Leningrad, 1978), 157 pp.
26. I.P. Mazin and A.Kh. Khrgian, eds., *Handbook of Clouds and Cloudy Atmosphere* (Gidrometeoizdat, Leningrad, 1989), 647 pp.
27. G.N. Glazov and G.A. Titov, *Izv. Vyssh. Uchebn. Zaved. Ser. Fizika*, No. 9, 151-154 (1975).
28. G.A. Mikhailov, *Optimization of the Weighting Monte Carlo Methods* (Nauka, Moscow, 1987), 238 pp.